Total Ozone from the Ozone Monitoring Instrument (OMI) using the DOAS Technique

J. P. Veefkind, J. F. de Haan, E. J. Brinksma, M. Kroon and P. F. Levelt

Abstract— This paper describes the algorithm for deriving the total column of ozone from spectral radiances and irradiances measured by the Ozone Monitoring Instrument (OMI) on the EOS-Aura. The algorithm is based on the Differential Optical Absorption Spectroscopy (DOAS) technique. The main characteristics of the algorithm are described as well as an error analysis. The algorithm has been successfully applied to the first available OMI data. Initial validation results are very encouraging and clearly show the potential of the method.

***Index Terms*—Ozone, Remote sensing, Satellites applications, Terrestrial atmosphere**

I. Introduction

On July 15, 2004 the Ozone Monitoring Instrument (OMI) on board of the NASA EOS Aura satellite was launched. The OMI is the first of a new generation of space borne spectrometers that combine a high spatial resolution (13x24 km^2 at nadir with daily global coverage [Levelt et al., 2005a]. Measuring the trend in stratospheric ozone as well as detecting tropospheric ozone on regional scales are top priorities of the science objectives for the Aura satellite [Levelt et al., 2005b].

Space measurements of the ozone column have been performed operationally since the 1970s with the SBUV and TOMS series of instruments [Heath and Park, 1978]. These measurements have played a major role in atmospheric chemistry, for example by monitoring the ozone layer [Chipperfield et al., 2003], as tracer for measuring stratospheric dynamics [e.g. Steinbrecht et al., 1998] and by detecting tropospheric ozone pollution on a regional scale [Fishman et al., 1990]. The original SBUV and TOMS instruments measure the backscattered radiance in a few 1 nm wide bands. From these bands, the ozone column is derived using radiances measured at two wavelengths, while other wavelengths are used for diagnostics and error correction [Bhartia and Wellemeyer., 2002; Bhartia et al., 2004]. In 1995 the GOME instrument was launched. It is the first of a series of space instruments that measure the ultra-violet and visible part of the spectrum with a high spectral resolution. In 2002 the SCIAMACHY instrument was launched, followed by OMI in 2004. These spectrometers make it possible to derive the ozone column using Differential Absorption Spectroscopy (DOAS) [Spurr et al., 1994; Burrows et al., 1999; Piters et al., 2000]. DOAS was developed for ground based measurements of atmospheric trace gases [Platt, 1994], but can also be applied to measurements from space. DOAS derives the ozone column by fitting a reference ozone absorption cross-section to the measured sun-normalized radiance. The main advantages of DOAS compared to the original SBUV/TOMS techniques are that DOAS is less sensitive to the radiometric calibration of the instrument and less sensitive to disturbing factors like absorbing aerosols. In this paper the implementation of the DOAS technique for measuring total ozone is described. First results of applying the algorithm to OMI data are presented, as well as first validation results using ground-based data.

Manuscript received xxxxx x, xxxx. This work was sponsored by NIVR, FMI

All authors are with the Royal Netherlands Meteorological Institute (KNMI), De Bilt, The Netherlands (phone: +31-30-2206-445; fax: +31-30-2210-407; e-mail: veefkind@knmi.nl).

II. Algorithm Description

The OMI total ozone DOAS algorithm consists of a three-step algorithm. First, the DOAS method is used to fit the differential absorption cross-section of ozone to the measured Sun-normalized Earth radiance spectrum, to obtain the so-called slant column density. In the second step the slant column density is translated into the vertical column density using the so-called air mass factor. The third step consists of a correction for cloud effects, to account for ozone that is hidden beneath the clouds. In this section we describe these steps, including the physical background, as well as assumptions and *a priori* information used.

A. Step 1: Deriving the Slant Column Density

The first step in the ozone DOAS algorithm is to determine the slant column density. The slant column density is determined by fitting an analytical function to the measured Earth radiance and solar irradiance data. This fit is applied to data taken in a certain wavelength range, called the fit window. A polynomial function, which serves as a high-pass filter, is applied to account for scattering and absorption that vary gradually with the wavelength, e.g., reflection by the surface and scattering by molecules, aerosols, and clouds. Also, the low pass filter takes out gradually varying radiometric calibration errors. The slant column density is derived from the filtered data, which contains spectral features of ozone in the fit window. It is the amount of ozone along an average path that the photons within the fit window travel from the Sun, through the atmosphere, to the satellite sensor. Figure 1 shows a DOAS fit applied to OMI data. The fit

function that is used in the OMI algorithm is based on the following equation:

$$\frac{I(\lambda)}{F(\lambda)} = P(\lambda)\exp\left[-N_s\,\sigma_{O3}(\lambda,T)\right], \quad (1)$$

where I is the radiance; F is the extraterrestrial solar irradiance; P is a low order polynomial; N_s is the ozone slant column density; σ_{O3} is the absorption cross section of ozone; and λ is the wavelength. To properly account for temperature effects the effective ozone temperate is derived from the DOAS fit itself. This is done by writing the ozone absorption cross section in equation 1 as:

$$\sigma_{O3}(\lambda,T) = \sigma_{O3}(\lambda,T_0) + (T-T_0)\left.\frac{d\sigma_{O3}(\lambda)}{dT}\right|_{T=T_0}. \quad (2)$$

Equation 1 is only accurate when dealing with elastic scattering. However, approximately 8% of the light scattering events in the OMI fit window is inelastic, meaning that the emission is at a different wavelength than the incoming light. The effect of this inelastic rotational Raman scattering is that structures in the spectrum are reduced. This holds for Fraunhofer structures (the well-known Ring effect) as well as for spectral structures caused by absorption in the atmosphere. Because Raman scattering reduces spectral structures, not accounting for it properly can cause an underestimation of the slant column density of the order 3 to 10 % [Valks, 2003]. When including terms that account for Raman scattering, the fit function can be expressed as:

$$\frac{I(\lambda)}{F(\lambda)} = P(\lambda)\,\exp\left[-N_s\,\sigma_{O3}(\lambda,T)\right] + c_{Ring}\frac{I_{Ring}(\lambda)}{F(\lambda)}\exp\left[-N_s\,\sigma'_{O3}(\lambda,T)\right], \quad (3)$$

where I_{Ring} is the extraterrestrial solar irradiance convoluted with the Raman lines; c_{Ring} is fit parameter to scale the radiance due to Raman scattering; and $\_'_{O3}$ is the ozone absorption cross section partly scrambled by Raman scattering. This ozone cross section is computed for a geometrical path through the atmosphere where all scattering takes place below the ozone absorption.

The fit parameters of equation 3 (N_s, T, c_{Ring}, and the polynomial coefficients) are determined using a non-linear least-squares fit. Information on the quality of the fit and the fit parameters is derived from the covariance matrix.

Detailed studies were performed to find the optimum fit window for ozone. The conclusions of these studies are that the main drivers for the fit window are the sensitivity of the slant column density to the atmospheric temperature and to the instrument signal-to-noise. The temperature effects are smallest in the parts of the spectrum were the correlation between the high-pass filtered ozone cross section and its derivative to the temperature is minimal. The signal-to-noise effects put a minimum on the width of the fit window. Based on these considerations a 5 nm wide window centered around 334.1 nm was selected as the default for OMI.

B. Step2: Air Mass Factor Correction

In DOAS the air mass factor is used to translate the slant column density into a vertical column density. The air mass factor M is defined as the ratio of the slant column density, N_s, and the vertical column density, N_v. From this definition it follows that M will depend on the viewing and solar geometry, the fit window used, the surface albedo, surface pressure, the actual ozone profile, clouds and aerosols, as they all affect the amount of ozone along the average photon path. The air mass factor is computed by simulating the measured spectra and applying DOAS to this simulated spectrum. For the simulations of the measured OMI spectrum a radiative transfer models is used, in combination with a simple OMI simulator. The OMI simulator is used to translate the high-resolution spectra from the radiative transfer model into spectra on the OMI spectral resolution and sampling. On the simulated spectra the DOAS fit function is applied to compute the slant column density. Since for the simulated spectra the vertical column density is known, the air mass factor can be computed as $M = N_s / N_v$. The calculated air mass factor is accurate if the model atmosphere used in the radiative transfer calculations resembles the actual atmosphere.

The air mass factor is pre-computed and stored in look-up tables as a function of the Sun/satellite geometry, the surface pressure and albedo, latitude, month, and total ozone amount. The ozone profiles are based on the TOMS V8 ozone climatology [Bhartia and Wellemeyer, 2002]. The surface albedo is derived by combining the TOMS surface albedo climatology [Herman and Celarier, 1999] with actual snow cover and sea ice coverage information. Figure 2 shows the dependence of the air mass factor on the ozone profile, if no *a priori* information was used. This figure shows that the dependence is largest for ozone hole conditions, whereas the dependence on Solar zenith angle is very weak. To reduce the uncertainty in the air mass factor due to the variations in the ozone profile, the appropriate profile is estimated based on the measured slant column density. To derive a relation between the slant column density and the ozone profile, a three ozone profiles are used that cover the natural variability of the ozone profile for a given location and time period. For each of these profiles the slant column density and air mass factor is calculated for a given Sun/satellite geometry, cloud condition and surface property. In this manner a relationship is derived between the air mass factor and the slant column density, as illustrated in Figure 3. The air mass factor to be applied to the measurement is computed by evaluating this relationship for the measured slant column density.

C. Step 3: Cloud Correction

When a ground pixel is (partly) covered by clouds, the algorithm has to account for the effects of clouds. Two kinds of effects are accounted for: firstly the effects of clouds on the air mass factor, and secondly the effect that clouds make part of the ozone column invisible for satellite instruments.

To calculate the air mass factor for cloudy conditions a cloud model is necessary. To determine the air mass factor for cloudy conditions, the cloud fraction and cloud pressure from

the OMI O_2-O_2 cloud product are used [Acarreta et al., 2004]. For consistency, it is important to use the same cloud model as used in the cloud product. This cloud model represents clouds by opaque Lambertian surfaces with an albedo of 0.80, placed at the cloud pressure. It was found by [Koelemeijer and Stammes, 1999] that this value for the cloud albedo gives the best results for ozone retrieval using DOAS. This cloud model considers all clouds to be thick, single layer clouds. Partly cloudy pixels are treated as the weighted sum of a clear and a cloudy pixel. Pixels that are fully covered with thin clouds are represented by partly cloudy pixels with a thick cloud. Using this cloud model, the air mass factors for fully cloudy conditions are determined in the same manner as those for clear ground pixels, which was described in the previous section. Partly cloudy ground pixels are treated as the weighted sum for clear and cloudy conditions:

$$M = w \cdot M_{cloudy} + (1 - w)\, M_{clear} \quad , \qquad (3)$$

where the weight w is the fraction of the radiance that is due to the cloudy part of the ground pixel.

The amount of ozone below the Lambertian cloud is called the "ghost column" and is computed by integrating the ozone profile from the surface to the cloud pressure. The profiles are taken from the TOMS V8 climatology [Bhartia and Wellemeyer, 2002]. Just as for the air mass factor, the appropriate profile, and hence, the appropriate ghost column is estimated using the measured slant column density. .

Finally, the vertical column amount N_v can be computed:

$$N_v = \frac{N_s + w \cdot M_{cloudy} \cdot N_g}{M} \quad , \qquad (4)$$

where N_g is the ghost column.

III. Error Analysis

During the development phase of the algorithm an extensive error analysis was performed to estimate the expected accuracy of the algorithm. This error analysis was described in [Veefkind and De Haan, 2002]. The focus of this error analysis was on the nominal cases. Exceptional cases, such as for example desert dust and polar stratospheric clouds were assessed separately. Table 1 summarizes the results from the error analysis for each of the algorithm steps. In this table a distinction is made between the total and the relative error. The relative errors are defined as errors that can vary for two measurements for the same location for two successive days. Thus, the systematic errors, which are not important for deriving trends, are excluded from the relative error. As can be seen in Table 1, the relative error of the vertical column density is 1.2 % for a cloud-free pixel, 2.2% for a cloudy pixel and 1.7% for a partly cloudy pixel. For cloudy conditions, the relative error is dominated by errors in the air mass factor related to clouds. For cloud-free conditions the error is dominated by the fitting of the slant column density. For trend analysis the instrument signal to noise error is not important, and for clear pixels the error is then dominated by the uncertainty in the ozone profile.

IV. First Results

From the beginning of October until the end of November 2004, OMI measured the Earth radiance almost continuously. This time period covers an important part of the Antarctic ozone hole for this year. Figure 4 shows an example of the total ozone derived for 1 November 2004, clearly showing the Antarctic ozone hole. This figure also illustrates the daily global coverage of the OMI instrument. To make a first assessment of the quality of the ozone data from the algorithm, a comparison was done with available Brewer stations in the Northern Hemisphere. It is noted that this exercise is the very beginning of the validation effort. As described in [Brinksma and McPeters, 2004], the core validation will include many more comparisons with all sorts of correlative data. However, the first comparisons show that the average bias of the OMI DOAS total ozone, as compared with the Brewer results, is 1.8 +/- 1.4 %, see Figure 5. The OMI data seem to be slightly higher than the Brewer observations. Although the reported difference is of the order of the expected accuracy, we believe that further improvement is possible. Apart from improvements in the (spectral) calibration of the instrument, improvements in the cloud correction part will become possible if better estimates of the cloud fraction become available.

V. Conclusion

In this paper the DOAS algorithm for deriving the total ozone column from OMI data was described and first results are presented. First comparisons with ground based observations for the Northern Hemisphere for a limited time period, show agreement within 2%. This is of the same order of magnitude as expected from an error analysis. However, still significant improvement of the OMI total ozone product is expected.

Acknowledgment

The authors like to thank Dimitris Balis from the Aristotle University of Thessaloniki for making the Brewer ozon data available to us.

References

[1] J. R. Acarreta, J. F. de Haan and P. Stammes, "Cloud pressure retrieval using the O2-O2 absorption band at 477 nm", *JGR, Vol 109, D05204*, doi: 10.1029/2003JD003915, 2004.

[2] A. M. Bass and R. J. Paur, "The ultraviolet cross-sections of ozone. I. The measurements. II - Results and temperature dependence", in *Proc. Quadrennial Ozone Symp.*, Eds. C. Zefros and A. Ghazi, Dordrecht, pp. 606, 1986.

[3] P. K. Bhartia and C. Wellemeyer, "TOMS-V8 Total O3 Algorithm", in OMI ATBD, Volume II, OMI Ozone Product", P. K. Bhartia, Ed., NASA GSFC, Greenbelt, MD, OMI-ATBD-02, pp 15-31, 2002.

[4] P. K. Bhartia, R. D. McPeters, L. E. Flynn and C. G. Wellemeyer, "Highlights of the Version 8 SBUV and TOMS Datasets Released at this Symposium", in *Proc. Quadrennial Ozone Symp.*, Ed. C. Zefros Athens, pp. 294, 2004.

[5] E. J. Brinksma and R. McPeters, "Ozone Column Workpackage", in *Ozone Monitoring Instrument Detailed Validation Handbook*, M. Kroon and E.J. Brinksma, Eds., KNMI, De Bilt, The Nethherlands, Tech. Note TN-KNMI-OMIE-583, 2004.

[6] J. P. Burrows, M. Weber, M. Buchwitz, V. Rozanov, A Ladstätter-Weissenmayer, A. Richter, R. De Beek, R. Hoogen, K. Bramstedt,

K.W. Eichmann, M. Eisinger, and D. Perner, "The Global Monitoring Experiment (GOME): Mission concept and first scientific results", *J. Atmos Sci., Vol 56*, pp. 151-175, 1999.

[7] M. P. Chipperfield, W.J. Randel and co-authors, "Global Ozone Past and Future", in: *Scientific assessment of ozone depletion: 2002*, WMO, Geneva, Switserland, pp. 4.1-4.90, March 2003.

[8] J. Fishman, C.E. Watson, J. C. Larsen, and J. A. Logan, "Distribution of tropospheric ozone determined from satellite data", *J. Geophys. Res., 95*, pp. 3599-3617, 1990.

[9] D. F. Heat and H. Park, "The Solar Backscatter Ultraviolet (SBUV) and Total Ozone Mapping Spectrometer (TOMS) Experiment", in: *The Nimbus-7 Users Guide*, C. R. Madrid, Ed., NASA Goddard Space Flight Center, Greenbelt, MD, pp. 175-211, 1978.

[10] J. R. Herman and E.A. Celarier, "Earth surface reflectivity climatology at 340-380 nm from TOMS data", *J. Geophys. Res., Vol 102*, pp. 28003-28011, 1997.

[11] R. B. A. Koelemeijer and P. Stammes, "Effects of clouds on ozone column retrieval from GOME UV measurements", J. *Geophys. Res., Vol 104, NO. D7*, pp. 8,281- 8,294, 1999.

[12] P. F. Levelt and co-authors, "The Ozone Monitoring Instrument", *IEEE Trans. Geo. Rem. Sens.*, this issue, 2005a.

[13] P. F. Levelt, E. Hilsenrath, G.W. Leppelmeier. G. B. J. van den Oord, P. K. Bhartia, and J. Tamminen. "Science Objectives of the Ozone Monitoring Instrument", *IEEE Trans Geo. Rem. Sens*. this issue, 2005b

[14] A. J M. Piters, P. J. M. Valks, R. B. A. Koelemeijer and D. M. Stam, "GOME Ozone Fast Delivery and value-Added Products, Version 3.0", KNMI, De Bilt, The Netherlands, Rep. GOFAP-KNMI-ASD-01, 2000.

[15] U. Platt, U., "Differential Optical Absorption Spectroscopy (DOAS)", in *Air Monitoring by Spectroscopic Techniques*, M. W. Sigrist, Ed., New York: Wiley & Sons, 1994, pp. 27-84.

[16] R. Spurr, "GOME Level 1 to 2 Algorithms Description", DLR, Oberpfaffenhofen, Germany, Technical Note ER-TN-DLR-GO-0025, 1994.

[17] W. Steinbrecht, H. Claude, U. Köhler and K. P. Hoinka, "Correlations between tropopauuse height and total ozone: Implications for long-term changes", *J. Geophys. Res., Vol 103 No. D5*, pp 19,183-19,192, 1998.

[18] P. J. M. Valks, "Retrieval of total and tropospheric ozone from observations by the Global Ozone Monitoring Experiment", Ph.D. dissertation, Dept. Physics., Eindhoven Tech. Univ., Eindhoven, 2003.

[19] J. P. Veefkind and J. F. de Haan, "DOAS Total O3 algorithm", in OMI ATBD, Volume II, OMI Ozone Product", P. K. Bhartia, Ed., NASA GSFC, Greenbelt, MD, OMI-ATBD-02, pp. 33-49, 2002.

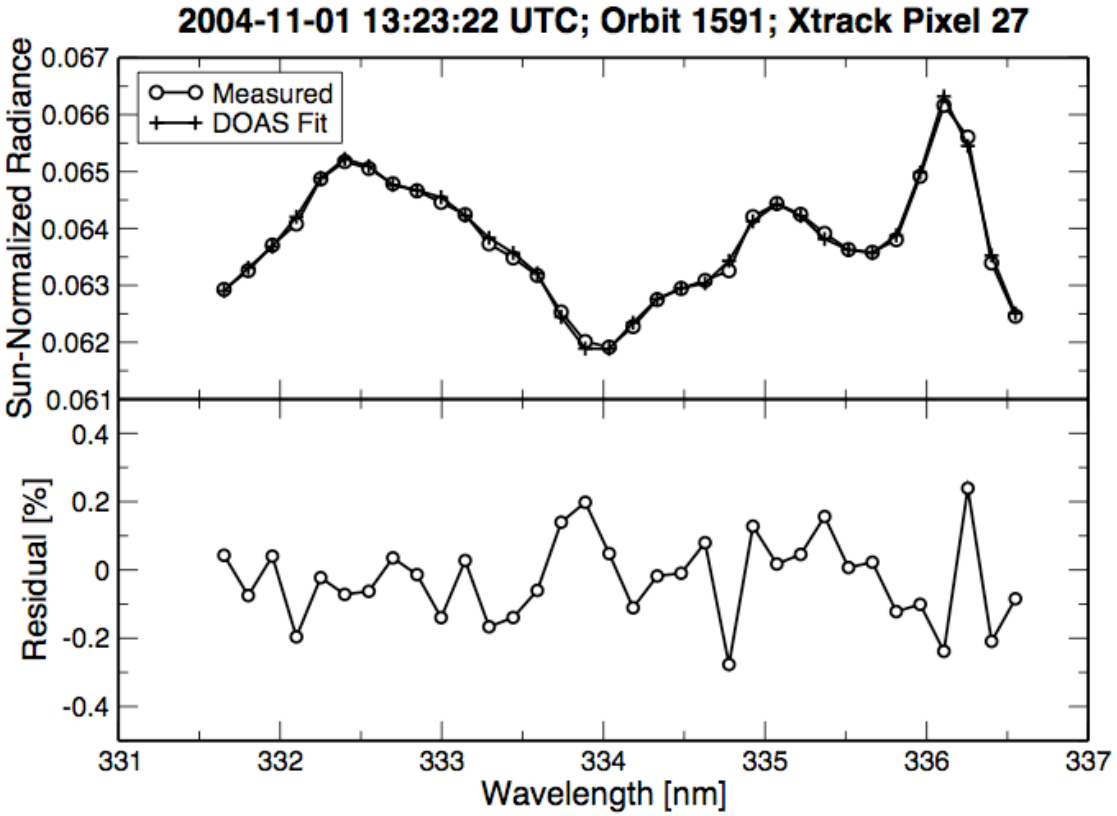

Figure 1. Example of a DOAS fit on OMI data measured 1 November 2004 13:23:32 UTC. The upper panel shows the measured Sun normalized radiance and the result of the DOAS fit. The lower panel show the residual between measurement and fit, expressed as the relative difference between the two.

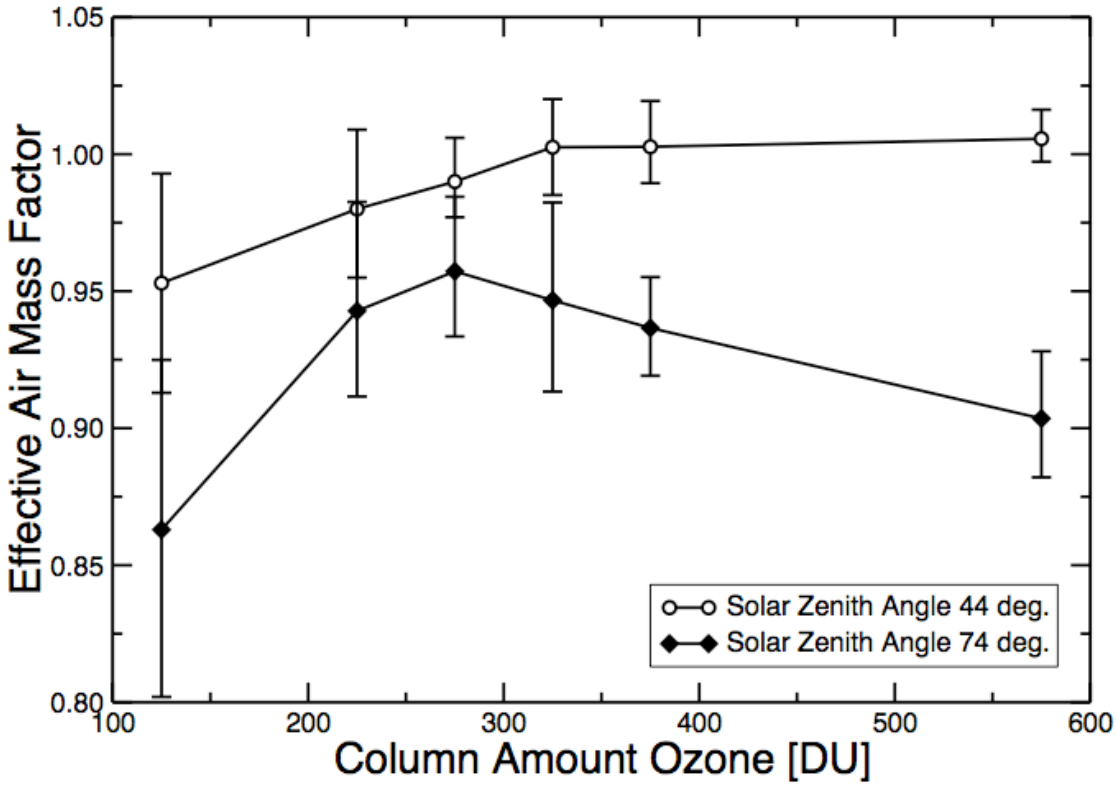

Figure 2. The effective air mass factor as a function of the total ozone column for two Solar zenith angles. Each of the lines shows the result of 648 profiles derived from the TOMS V8 ozone profile climatology. The symbols show the mean effective air mass factor at specific column amount ozone, the bars show the minimum and maximum values. The Solar zenith angles are 44 and 74 degrees, the viewing angle is 33 degrees, the relative azimuth angle is 90 degrees and the surface albedo 0.1.

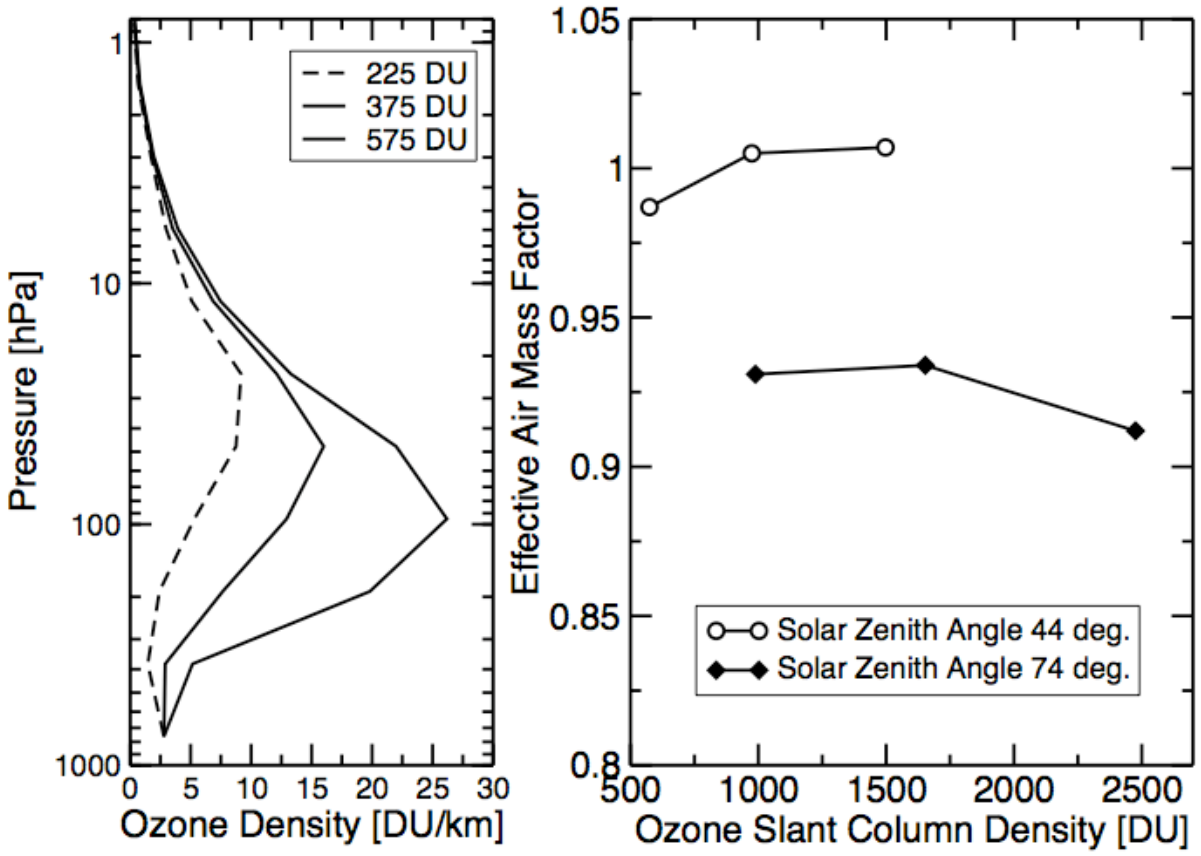

Figure 3. Left panel: Ozone profiles from the TOMS Version 8 climatology for 55° N for December, with a total column of ozone of 225, 375 and 575 DU. Right panel shows the effective air mass factors as a function of the slant column density for two Sun-satellite geometries, as computed for the ozone profiles shown in the left panel. The Sun-satellite geometry are: solar zenith angle 44 and 74 degrees; viewing zenith angle 34 degrees; and relative azimuth angle 90 degrees. The surface albedo is 0.1.

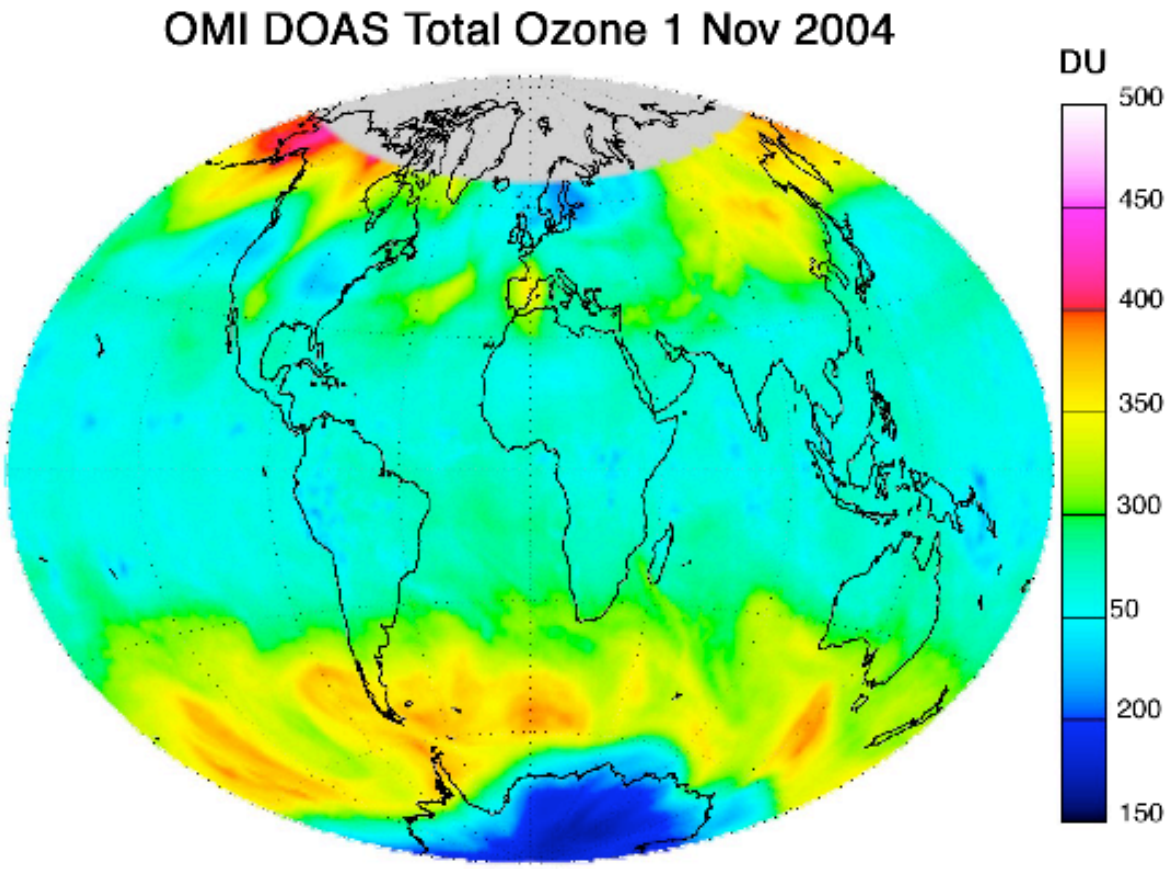

Figure 4. Total ozone column for 1 November 2004, derived using the OMI DOAS algorithm.

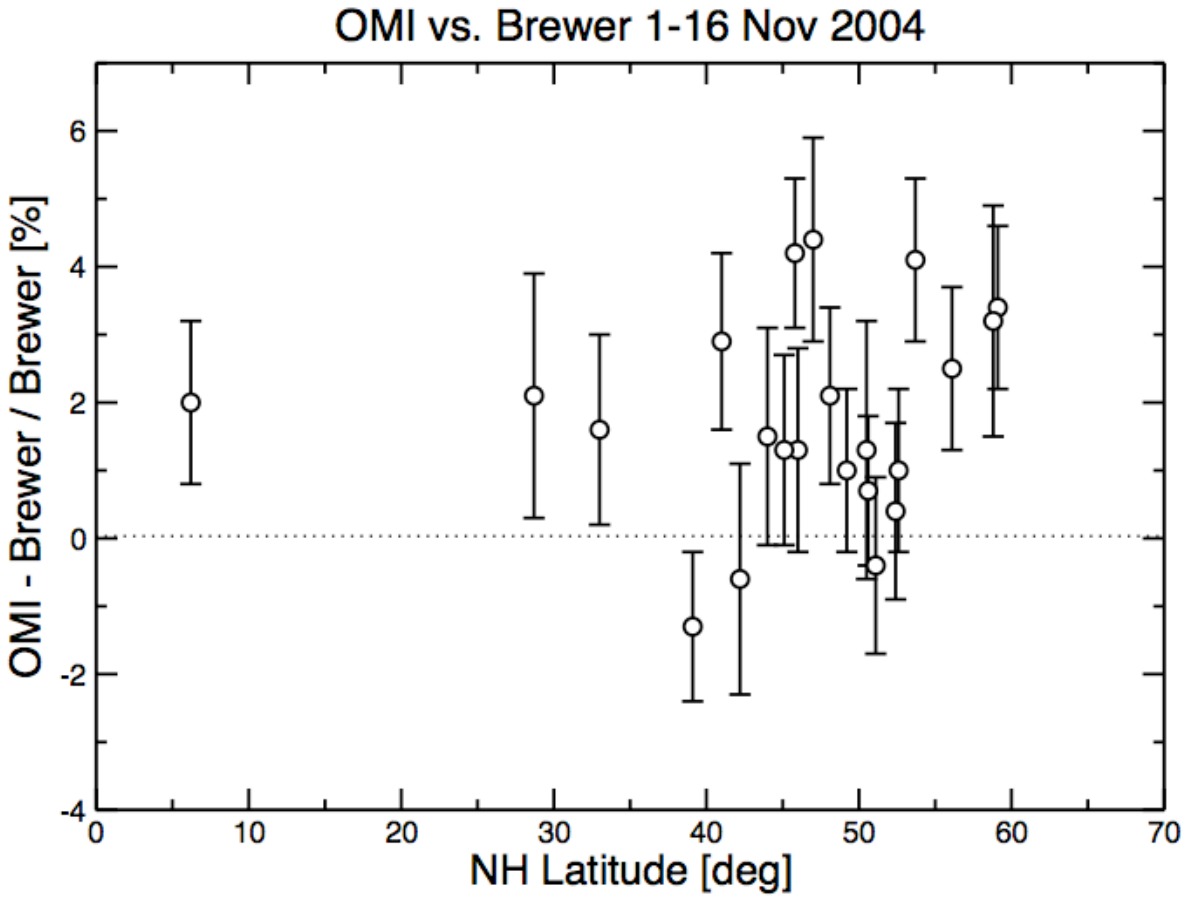

Figure 5. Comparisons between the OMI total ozone column from the DOAS algorithm and selected Brewer stations in the Northern Hemisphere, for the period 1-16 November 2004. OMI data points co-located within 50 km and 1 hour are included in this figure.

TABLE 1
ERROR ESTIMATES FOR THE OMI OZONE DOAS PRODUCT.

Source	Total Error [%]	Relative Error [%]
Slant Column Density		
Other trace gases	0.5	
Absorption cross section	1	
Instrument response function	0.1	
Atmospheric temperature	0.3	0.3
Instrument signal-to-noise	1	1
Instrument spectral calibration	1	
Instrument spectral stability	0.25	
Air mass factor		
Aerosols	0.2	0.2
Cloud Model	1	1
Ozone profile	0.5	0.5
Surface reflectivity	0.3	
Cloud pressure	1	1
Cloud fraction	0.8	0.8
Cloud Correction		
ghost column	40	40
Vertical Column Density		
Clear	2.1	1.2
Partly Cloudy	2.5	1.7
Cloudy	3.0	2.2